

The Astrocyte as a Gatekeeper of Synaptic Information Transfer

Vladislav Volman¹, Eshel Ben-Jacob^{1,2} & Herbert Levine²

¹ School of Physics and Astronomy, Raymond and Beverly Sackler Faculty of Exact Sciences,
Tel-Aviv Univ., 69978, Tel-Aviv, Israel

² - Center for Theoretical Biological Physics, University of California at San Diego,
La Jolla, CA 92093-0319 USA

e-mails: volman(at)salk.edu, eshel(at)tamar.tau.ac.il, hlevine(at)ucsd.edu

February 9, 2008

Abstract

We present a simple biophysical model for the coupling between synaptic transmission and the local calcium concentration on an enveloping astrocytic domain. This interaction enables the astrocyte to modulate the information flow from presynaptic to postsynaptic cells in a manner dependent on previous activity at this and other nearby synapses. Our model suggests a novel, testable hypothesis for the spike timing statistics measured for rapidly-firing cells in culture experiments.

Introduction

In recent years, evidence has been mounting regarding the possible role of glial cells in the dynamics of neural tissue [1, 2, 3, 4]. For astrocytes in particular, the specific association of processes with synapses and the discovery of two-way astrocyte-neuron communication has demonstrated the inadequacy of the previously-held view regarding the purely supportive role for these glial cells. Instead, future progress requires rethinking how the dynamics of the coupled neuron-glial network can store, recall, and process information.

At the level of cell biophysics, some of the mechanisms underlying the so-called "tripartite synapse" [5] are becoming more clear. For example, it is now well-established that astrocytic mGlu receptors detect synaptic activity and respond via activation of the calcium-induced calcium release pathway, leading to elevated Ca^{2+} levels. The spread of these levels within a micro-domain of one cell can coordinate the activity of disparate synapses that are associated with the same micro-domain [6]. Moreover, it might even be possible to transmit information directly from domain to domain and even from astrocyte to astrocyte, if the excitation level is strong enough to induce either intracellular or intercellular calcium waves [7, 8, 9]. One sign of the maturity in our understanding is the formulation of semi-quantitative models for this aspect of neuron-glial communication [10, 11, 12].

There is also information flow in the opposite direction, from astrocyte to synapse. Direct experimental evidence for this, via the detection of the modulation of synaptic transmission as a function of the state of the glial cells will be reviewed in more detail below. One of the major goals of this work will be to introduce a simple phenomenological model for this interaction. The model will take into account both a deterministic effect of high Ca^{2+} in the astrocytic process, namely the reduction of the post-synaptic response to incoming spikes on the presynaptic axon [13], and a stochastic effect, namely the increase in the frequency of observed miniature post-synaptic current events uncorrelated with any input [14]. There are also direct NMDA-dependent effects on the postsynaptic neuron of astrocyte-emitted factors [15], which are not considered here.

As we will show, the aforementioned coupling allows the astrocyte to act as a "gatekeeper" for the synapse. By this, we mean that the amount of data transmitted across the synapse can be modulated by astrocytic dynamics. These dynamics may be controlled mostly by other synapses, in which case the gate-keeping will depend on dynamics external to the specific synapse under consideration. Alternatively, the dynamics may depend mostly on excitation from the selfsame synapse, in which case the behavior of the entire system is determined self-consistently. Here we will focus on the latter possibility and leave for future work the discussion of how this mechanism could lead to multi-synaptic coupling

Our ideas regarding the role of the astrocyte are utilized to offer a new explanation for observations regarding firing patterns in cultured neuronal networks. In particular, spontaneous bursting activity in these networks is regulated by a set of rapidly firing neurons which we refer to as "spikers"; these neurons exhibit spiking even during long inter-burst intervals and hence must have some form of self-consistent self-excitation. We model these neurons as containing astrocyte-mediated self-synapses (autapses) (see [16, 17, 18]) and show that this hypothesis naturally accounts for the observed unusual inter-spike interval distribution. Additional tests of this hypothesis will be proposed at the end.

Experimental observations

Cultured neuronal networks: The cultured neuronal networks presented here are self-generated from dissociated cultures of mixed cortical neurons and glial cells drawn from one-day-old Charles River rats. The dissection, cell dissociation and recording procedures were previously described in detail [19]. Briefly, following dissection, neurons are dispersed by enzymatic treatment and mechanical dissociation. Then the cells are homogeneously plated on multi electrode arrays (MEA, Multi-Channel Systems), pre-coated with Poly-L-Lysine. Culture media was DMEM, (sigma) enriched by serum and changed every two days. Plated cultures are placed on the MEA board (B-MEA-1060, Multi Channel Systems) for simultaneous long-term noninva-

sive recordings of neuronal activity from several neurons at a time. Recorded signals are digitized and stored for off-line analysis on a PC via an A-D board (Microstar DAP) and data acquisition software (Alpha-Map, Alpha Omega Engineering). Non-invasive recording of the networks activity (action potentials) is possible due to the capacitive coupling that some of the neurons form with some of the electrodes. Since typically one electrode can record signals from several neurons, a specially developed spike-sorting algorithm [20] is utilized to reconstruct *single* neuron-specific spike series. Although there are no externally provided guiding stimulations or chemical cues, relatively intense dynamical activity is spontaneously generated within several days. The activity is marked by the formation of synchronized bursting events (SBEs) short (200ms) time windows during which most of the recorded neurons participate in relatively rapid firing [21]. These SBEs are separated by long intervals (several seconds or more) of sporadic neuronal firing of most of the neurons. A few neurons (referred to as spiker neurons) exhibit rapid firing even during the inter SBEs time intervals. These neurons also exhibit much faster firing rates during the SBEs and their inter-spike-intervals distribution is marked by a long tail behavior (see Fig. 4).

Inter-spike interval (ISI) increments distribution: One of the tools used to compare model results with measured spike data concerns the distribution of increments in the spike times, defined as $\delta(i) = ISI(i+1) - ISI(i), i \geq 1$. The distribution of $\delta(i)$ will have heavy tails if there are a wide range of inter-spike intervals and if there are rapid transitions from one type of interval to the next. For example, rapid transitions from bursting events to occasional inter-burst firings will lead to such a tail. Applying this analysis to the recorded spike data of cultured cortical networks, Segev et al. [19] found that distributions of neurons ISI increments can be well-fitted with Levy functions over 3 decades in time.

The model

In this section we present the mathematical details of the models which will be employed in this work. Readers interested mainly in the conclusions can

skip directly to the Results section.

The basic notion we use is that standard synapse models must be modified to account for the astrocytic modulation, depending of course on the calcium level. In turn, the astrocytic calcium level is affected by synaptic activity; for this we use the Li-Rinzel model where the IP_3 concentration parameter governing the excitability is increased upon neurotransmitter release. These ingredients suffice to demonstrate what we mean by gate-keeping. Finally, we apply this model to the case of an autaptic oscillator, which requires the introduction of neuronal dynamics. For this, we chose the Morris-Lecar model as a generic example of a type-I firing system. None of our results would be altered with a different choice, as long as we retain the tangent-bifurcation structure which allows for arbitrarily long inter-spike intervals. Now for the details:

TUM Synapse Model: To describe the kinetics of a synaptic terminal, we have used the model of an activity-dependent synapse first introduced by Tsodyks, Uziel and Markram [22]. In this model, the effective synaptic strength evolves according to the following equations :

$$\begin{aligned}\dot{x} &= \frac{z}{\tau_{rec}} - ux\delta(t - t_{sp}) \\ \dot{y} &= -\frac{y}{\tau_{in}} + ux\delta(t - t_{sp}) \\ \dot{z} &= \frac{y}{\tau_{in}} - \frac{z}{\tau_{rec}}\end{aligned}\tag{1}$$

Here, x , y , and z are the fractions of synaptic resources in the recovered, active and inactive states, respectively. For an excitatory glutamatergic synapse, the values attained by these variables can be associated with the dynamics of vesicular glutamate. As an example, the value of y in this formulation will be proportional to the amount of glutamate that is being released during the synaptic event, and the value of x will be proportional to the size of readily releasable vesicle pool. The time-series t_{sp} denote the arrival times of pre-synaptic spikes, τ_{in} is the characteristic time of post-synaptic currents (PSCs) decay, and τ_{rec} is the recovery time from synaptic depression. Upon arrival of a spike to the pre-synaptic terminal at time t_{sp} , a fraction u of available synaptic resources is transferred from the recovered state to the

active state. Once in the active state, synaptic resource rapidly decays to the inactive state, from which it recovers within a time-scale τ_{rec} . Since the typical times are assumed to satisfy $\tau_{rec} \gg \tau_{in}$, the model predicts onset of short-term synaptic depression after a period of high-frequency repetitive firing. The onset of depression can be controlled by the variable u , which describes the effective use of synaptic resources by the incoming spike. In the original TUM model, the variable u is taken to be constant for the excitatory post-synaptic neuron; in what follows we will set $u = 0.1$. Other parameter choices for these equations as well as for the rest of the model equations are presented in the accompanying table.

To complete the specification, it is assumed that the resulting post-synaptic current (PSC), arriving at the model neurons' soma through the synapse depends linearly on the fraction of available synaptic resources. Hence, a total synaptic current seen by a neuron is $I_{syn}(t) = Ay(t)$, where A stands for an absolute synaptic strength. At this stage, we do not take into account the long-term effects associated with the plasticity of neuronal somata and take the parameter A to be time-independent.

Astrocyte response: Astrocytes adjacent to synaptic terminals respond to the neuronal action potentials by binding glutamate to their metabotropic glutamate receptors [23]. The activation of these receptors then triggers the production of IP_3 , which, consequently, serves to modulate the intracellular concentration of calcium ions; the effective rate of IP_3 production depends on the amount of transmitter that has been released during the synaptic event.

We therefore assume that the production of intracellular IP_3 in the astrocyte is given by

$$\frac{d[IP_3]}{dt} = \frac{IP_3^* - IP_3}{\tau_{ip_3}} + r_{ip_3}y \quad (2)$$

The above equation is similar to the formulation used by Nadkarni and Jung [10], with some important differences. First, the effective rate of IP_3 production depends not on the potential of neuronal membrane, but on the amount of neurotransmitter that is being released into the synaptic cleft. Hence, as the resources of synapse are depleted (due to depression), there will be less transmitter released, and, therefore, the IP_3 will be produced at lower

rates, leading eventually to decay of calcium concentration. Second, as the neuro-transmitter is released also during spontaneous synaptic events (noise), the latter will also influence the production of IP_3 and subsequent calcium oscillations.

Astrocyte: To model the dynamics of a single astrocytic domain, we use the Li-Rinzel model [24, 10], which has been specifically developed to take into account the IP_3 -dependent dynamical changes in the concentration of cytosolic Ca^{2+} . This is based on the theoretical studies of Nadkarni and Jung [10], where it is decisively demonstrated that astrocytic Ca^{2+} oscillations may account for the spontaneous activity of neurons.

The intracellular concentration of Ca^{2+} in the astrocyte is described by the following set of equations:

$$\frac{d[Ca^{2+}]}{dt} = -J_{chan} - J_{pump} - J_{leak} \quad (3)$$

$$\frac{dq}{dt} = \alpha_q(1 - q) - \beta_q q \quad (4)$$

Here, q is the fraction of activated IP_3 receptors. The fluxes of currents through ER membrane are given in the following expressions:

$$J_{chan} = c_1 v_1 m_\infty^3 n_\infty^3 q^3 ([Ca^{2+}] - [Ca^{2+}]_{ER}) \quad (5)$$

$$J_{pump} = \frac{v_3 [Ca^{2+}]^2}{k_3^2 + [Ca^{2+}]^2} \quad (6)$$

$$J_{leak} = c_1 v_2 ([Ca^{2+}] - [Ca^{2+}]_{ER}) \quad (7)$$

where

$$m_\infty = \frac{[IP_3]}{[IP_3] + d_1} \quad (8)$$

$$n_\infty = \frac{[Ca^{2+}]}{[Ca^{2+}] + d_5} \quad (9)$$

$$\alpha_q = a_2 d_2 \frac{[IP_3] + d_1}{[IP_3] + d_3} \quad (10)$$

$$\beta_q = a_2 [Ca^{2+}] \quad (11)$$

The reversal Ca^{2+} concentration ($[Ca^{2+}]_{ER}$) is obtained after requiring conservation of the overall Ca^{2+} concentration:

$$[Ca^{2+}]_{ER} = \frac{c_0 - [Ca^{2+}]}{c_1} \quad (12)$$

Glia-synapse interaction: Astrocytes affect synaptic vesicle release in a calcium dependent manner. Rather than attempt a complete biophysical model of the complex chain of events leading from calcium rise to vesicle release [25], we proceed in a phenomenological manner. We define a dynamical variable f which phenomenologically will capture this interaction; when the concentration of calcium in its synapse-associated process exceeds a threshold, we assume that the astrocyte emits a finite amount of neurotransmitter into the peri-synaptic space, thus altering the state of a nearby synapse; this interaction occurs via glutamate binding to pre-synaptic mGlu and NMDA receptors [26]. As the internal astrocyte resource of neurotransmitter is finite, we include saturation term $(1 - f)$ in the dynamical equation for f . The final form is

$$\dot{f} = \frac{-f}{\tau_{Ca^{2+}}} + (1 - f)\kappa\Theta([Ca^{2+}] - [Ca_{threshold}^{2+}]) \quad (13)$$

Given this assumption, equations 1 should be modified to take this modulation into account. We assume the following simple form:

$$\dot{x} = \frac{z}{\tau_{rec}} - (1 - f)ux\delta(t - t_{sp}) - x\eta(f) \quad (14)$$

$$\dot{y} = \frac{-y}{\tau_{in}} + (1 - f)ux\delta(t - t_{sp}) + x\eta(f) \quad (15)$$

In the above equations, $\eta(f)$ represents a noise term modelling the increased occurrence of mini-PSC's. The fact that a noise increase accompanies an amplitude decrease is partially due to competition for synaptic resources between this two release modes [27]. Based on experimental observations, we prescribe that the dependence of $\eta(f)$ on f is such that rate of noise occurrence (the frequency of $\eta(f)$ in a fixed time step) increases with increasing f , but the amplitude distribution (modelled here as a Gaussian-distributed

variable centered around positive mean) remains unchanged. For the rate of noise occurrence, we chose the following functional dependence:

$$P(f) = P_0 \exp\left(-\left(\frac{1-f}{\sqrt{2}\sigma}\right)^2\right) \quad (16)$$

with P_0 representing the maximal frequency of $\eta(f)$ in a fixed time step.

Note that although both synaptic terminals and astrocytes utilize glutamate for their signaling purposes, we assume the two processes to be independent. In so doing, we rely on the existing biophysical experiments which demonstrate that, whereas a presynaptic terminal releases glutamate in the synaptic cleft, astrocytes selectively target extra-synaptic glutamate receptors [13, 14]. Hence, synaptic transmission does not interfere with the astrocyte-to-synapse signalling.

Neuron model: We describe the neuronal dynamics with a simplified two-component Morris-Lecar model [28] :

$$\dot{V} = -I_{ion}(V, W) + I_{ext}(t) \quad (17)$$

$$\dot{W}(V) = \phi \frac{W_{\infty}(V) - W(V)}{\tau_W(V)} \quad (18)$$

with $I_{ion}(V, W)$ representing the contribution of the internal ionic Ca^{2+} , K^+ and leakage currents with their corresponding channel conductivities g_{Ca} , g_K and g_L being constant :

$$\begin{aligned} I_{ion}(V, W) = & g_{Ca}m_{\infty}(V)(V - V_{Ca}) + \\ & + g_KW(V)(V - V_K) + g_L(V - V_L) \end{aligned} \quad (19)$$

I_{ext} represents all the external current sources stimulating the neuron, such as signals received through its synapses, glia-derived currents, artificial stimulations as well as any noise sources. In the absence of any such stimulation, the fraction of open potassium channels, $W(V)$, relaxes towards its limiting curve (nullcline) $W_{\infty}(V)$, which is described by the sigmoid function :

$$W_{\infty}(V) = \frac{1}{2}\left(1 + \tanh\left(\frac{V - V_3}{V_4}\right)\right) \quad (20)$$

within a characteristic time scale given by :

$$\tau_W(V) = \frac{1}{\cosh(\frac{V-V_3}{2V_4})} \quad (21)$$

In contrast to this, it is assumed in the Morris-Lecar model that calcium channels are activated immediately. Accordingly, the fraction of open Ca^{2+} channels obeys the following equation :

$$m_\infty(V) = \frac{1}{2}(1 + \tanh(\frac{V - V_1}{V_2})) \quad (22)$$

For an isolated neuron, rendered with a single autapse, one has $I_{ext}(t) = I_{syn}(t) + I_{base}$ where $I_{syn}(t)$ is the current arriving through the self-synapse, and I_{base} is some constant background current. In this work, we assume that I_{base} is such that, when acting alone, it causes a neuron to fire at very low constant rate. Of course these two terms enter the equation additively and the dynamics just depends on the total external current. Nonetheless it is important to separate these terms as only one of them enters through the synapse; it is only this term that is modulated by astrocytic glutamate release and only this term that would be changed by synaptic blockers. As we will mention later, the baseline current may also be due to astrocytes, albeit to a direct current directed into the neuronal soma. In anticipation of a better future understanding of this term, we consider it separately from the constant appearing in leak current ($g_L V_L$) although there is clearly some redundancy in the way these two terms set the operating point of the neuron.

Results

Synaptic Model: In simple models of neural networks, the synapse is considered to be a passive element which directly transmits information, in the form of arriving spikes on the pre-synaptic terminal, to post-synaptic currents. It has been known for a long time that more complex synaptic dynamics can affect this transfer. One such effect concerns the finite reservoir of presynaptic vesicle resources and was modelled by Tsodyks, Uziel and Markram (TUM) [22]. Spike trains with too high a frequency will be attenuated by a TUM synapse, as there is insufficient recovery from one arrival to

the next. To demonstrate this effect, we fed the TUM synaptic model with an actual spike train recorded from a neuron in a cultured network (shown in Fig. 1a); the resulting post-synaptic current (PSC) is shown in Fig. 1b. As is expected there is attenuation of the PSC height during time windows with high rates of pre-synaptic spiking input.

The effect of pre-synaptic gating: Our goal is to extend the TUM model to include the interaction of the synapse with an astrocytic process imagined to be wrapped around the synaptic cleft. The effects of astrocytes on stimulated synaptic transmission are well-established. Araque *et al.* [13] report that astrocyte stimulation reduced the magnitude of action potential evoked excitatory and inhibitory synaptic currents by decreasing the probability of evoked transmitter release. Specifically, pre-synaptic metabotropic glutamate receptors (mGluRs) have been shown to affect the stimulated synaptic transmission by regulating pre-synaptic voltage-gated calcium channels which eventually leads to the reduction of calcium flux during the incoming spike and results in decrease of amplitude of synaptic transmission. These results are best shown in Fig. 8 of their paper, which presents the amplitude of evoked EPSC both before and after stimulation of an associated astrocyte. Note that we are referring here to “faithful” synapses, i.e. synapses that transmit almost all of the incoming spikes. Effects of astrocytic stimulation on highly stochastic synapses, namely the increase in fidelity [29], are not studied here.

In addition, astrocytes were shown to increase the frequency of spontaneous synaptic events. In detail, Araque *et al.* [14] have shown that astrocyte stimulation increases the frequency of miniature post-synaptic currents (mPSC), without modifying their amplitude distribution, suggesting that astrocytes act to increase the probability of vesicular release from the pre-synaptic terminal. Although the exact mechanism is unknown, this effect is believed to be mediated by NMDA receptors located at the pre-synaptic terminal. It is important to note that the two kinds of astrocytic influence on the synapse (decrease of the probability of evoked release and increase in the probability of spontaneous release) do not contradict each other. Evoked transmitter release depends on the calcium influx through calcium channels

that can be inhibited by the activation of pre-synaptic mGluRs. On the other hand, the increase in the probability of spontaneous release follows because of the activation of pre-synaptic NMDA channels. In addition, spontaneous activity can deplete the vesicle pool (either in terms of number or in terms of filling) and hence directly lower triggered release amplitudes [27].

We model these effects by two modifications of the TUM model. First, we introduce a gating function f which modulates the stimulated release in a calcium-dependent manner. This term will cause the synapse to turn off at high calcium. This pre-synaptic gating effect is demonstrated in Fig. 1c, where we show the resulting PSC corresponding to a case in which f is chosen to vary periodically with a time scale consistent with astrocytic calcium dynamics. The effect on the recorded spike train data is quite striking. The second effect, namely the increase of stochastic release in the absence of any input, is included as a f dependent noise term in the TUM equations. This will be important as we turn to a self-consistent calculation of the synapse coupled to a dynamical astrocyte.

The gate-keeping effect: We close the synapse-glia-synapse feedback loop by inclusion of the effect of the pre-synaptic activity on the intracellular Ca^{2+} dynamics in the astrocyte that in turn set the value of the gating function f . Nadkarni and Jung [10] have argued that the basic calcium phenomenology in the astrocyte, arising via the glutamate-induced production of IP_3 , can be studied via the Li-Rinzel model. What emerges from their work is that the dynamics of the intra-astrocyte Ca^{2+} level depends on the intensity of the pre-synaptic spike train, acting as an information integrator over a time scale on the order of seconds; the level of Ca^{2+} in the astrocyte increases according to the summation of the synaptic spikes over time. If the total number of spikes is low, the Ca^{2+} concentration in the astrocyte remains below a self-amplification threshold level and simply decays back to its resting level with some characteristic time. However, things change dramatically when a sufficiently intense set of signals arises across the synapse. Now, the Ca^{2+} concentration overshoots beyond its linear response level, followed by decaying oscillations.

Given our aforementioned results, these high Ca^{2+} levels in the astrocyte

will in fact attenuate spike information that arrives subsequent to strong bursts of activity. We illustrate this time-delayed gate-keeping (TDGK) effect in Fig. 2. We constructed a spike train by placing a time delay in between segments of recorded sequences. As can be seen, since the degree of activity during the first two segments exceeds the threshold level, there is attenuation of the late-arriving segments. Thus, the information passed through the synapse is modulated by previous arriving data.

Autaptic Excitatory Neurons: Our new view of synaptic dynamics will have broad consequences for making sense of neural circuitry. To illustrate this prospect, we turn to the study of an autaptic oscillator [30], by which we mean an excitatory neuron that exhibits repeated spiking driven at least in part by self-synapses [16, 17, 18, 31]. By including the coupling of a model neuron to our synapse system, we can investigate both the case of the role of an associated astrocyte with externally imposed temporal behavior and the case where the astrocyte dynamics is itself determined by feedback from this particular synapse. Finally, we should be clear that when we refer to one synapse, we are also dealing implicitly with the case of multiple self-synapses all of what are coupled to the same astrocytic domain which in turn is exhibiting correlated dynamics in its processes connecting to these multiple sites. It is important to note that this same modulation can in fact correlate multiple synapses connecting distinct neurons which are coupled to the same astrocyte. The effect of this new multi-synaptic coupling on the spatio-temporal flow of information in a model network will be described elsewhere.

We focus on an excitatory neuron modelled with Morris-Lecar dynamics, as described in Model section. We add some external bias current so as to place the neuron in a state slightly beyond the saddle-node bifurcation, to where it would spontaneously oscillate at a very low frequency in the absence of any synaptic input. We then assume that this neuron has a self-synapse (autapse). An excitatory self-synapse clearly has the possibility of causing a much higher spiking rate than would otherwise be the case; this behavior without any astrocyte influence is shown in Fig. 3. The existence of autaptic neurons was originally demonstrated in cultured networks [16, 18, 17], but

has been detected in intact neocortex as well [31]. Importantly, these can be either inhibitory or excitatory. There has been some speculation regarding the role of autapses in memory [30], but this is not our concern here.

Are such neurons observed experimentally? In Fig. 4 we show a typical raster plot recorded from cultured neural network grown from a dissociated mixture of glial and neuronal cortical cells taken from one day old Charles River rats (see Experimental Observations). The spontaneous activity of the network is marked by synchronized bursting events (SBEs) - short (several 100s of ms) periods during which most of the recorded neurons show relatively rapid firing separated by long (order of seconds) time intervals of sporadic neuronal firing of most of the neurons [21]. Only small fractions of special neurons (termed spiker neurons) exhibit rapid firing also during inter SBEs intervals. These spiker neurons also exhibit much higher firing rates during the SBEs. But the behavior of these rapid firing neurons do not match that expected of the simple autaptic oscillator. The major differences, as illustrated by comparing Figs. 3 and 4 are 1. the existence of long inter-spike-intervals for the spikers, marked by a long tail (Levy) distribution of the increments of the inter-spike intervals. 2. The beating or burst-like rate modulation in the temporal ordering of the spike train.

Motivated by the above and the glial gate-keeping effect studied earlier, we proceed to test if an autaptic oscillator with a glia-regulated self-synapse will bring the model into better agreement. In Fig. 5 we show that indeed the activity of such a modified model does show the additional modulation. The basic mechanism results from the fact that after a period of rapid firing of the neuron, the astrocyte intracellular Ca^{2+} concentration (shown in Fig. 5b) exceeds the critical threshold for time-delayed attenuation. This then stops the activity and gives rise to large inter-spike intervals. The distributions shown in Fig. 5 are a much better match to experimental data for time intervals up to 100 msec.

Robustness tests

The stochastic Li-Rinzel model: One of the implicit assumptions of our

model for astrocyte-synapse interaction is related to the deterministic nature of astrocyte calcium release. It is assumed that in the absence of any IP_3 signals from the associated synapses, the astrocyte will stay "silent", in the sense that there will be no spontaneous Ca^{2+} events. However, it should be kept in mind that the equations for the calcium channel dynamics used in the context of Li-Rinzel model, in fact describe the collective behavior of large number of channels. In reality, experimental evidence indicates that the calcium release channels in astrocytes are spatially organized in small clusters of 20-50 channels - the so-called "micro-domains". These micro-domains were found to contain small membrane leaflets (of $O(10nm)$ thick), wrapping around the synapses and potentially being able to synchronize ensembles of synapses. This finding calls for a new view of astrocytes as cells with multiple functional and structural compartments.

The micro-domains (within the same astrocyte) have been observed to generate the spontaneous Ca^{2+} signals. As the passage of the calcium ions through a single channel is subject to fluctuations, for small clusters of channels the stochastic aspects can become important. Inclusion of stochastic effects can explain the generation of calcium puffs - fast localized elevations of calcium concentration. Hence, it is important to test the possible effect of stochastic calcium events on the model's behavior.

We achieve this goal by replacing the deterministic Li-Rinzel model with its stochastic version, obtained using Langevin approximation, as has been recently described by Shuai and Jung [32]. With the Langevin approach, the equation for the fraction of open calcium channels is modified, and takes the following form:

$$\frac{dq}{dt} = \alpha_q(1 - q) - \beta_q q + \xi(t) \quad (23)$$

in which the stochastic term, $\xi(t)$, has the following properties:

$$\langle \xi(t) \rangle = 0 \quad (24)$$

$$\langle \xi(t)\xi(t') \rangle = \frac{\alpha_q(1 - q) + \beta_q q}{N} \delta(t - t') \quad (25)$$

In the limit of very large cluster size, $N \rightarrow \infty$, and the effect of stochastic Ca^{2+} release is not significant. On the contrary, the dynamics of calcium

release are greatly modified for small cluster sizes. A typical spike time-series of glia-gated autaptic neuron, obtained for the cluster size of $N = 10$ channels, is shown Fig. 6a. Note that, while there appear considerable fluctuations in concentration of astrocyte calcium (Fig. 6b), the dynamics of the gating function (Fig. 6c) is less irregular. This follows because our choice of the gating function corresponds to the integration of calcium events. We have also checked that the distribution of inter-spike-intervals are practically unchanged (data not shown). All told, our results indicate including the stochastic nature of the release of calcium from astrocyte ER does not affect the dynamics of our model autaptic neuron in any significant way.

The correlation time of the gating function: Another assumption made in our model concerns the dynamics of the gating function. We have assumed the simple first-order differential equation for the dynamics of our phenomenological gating function, and have selected time-scales that are believed to be consistent with the influence of astrocytes on synaptic terminals. However, because the exact nature of the underlying processes (and corresponding time-scales) is unknown, it is important to test the robustness of the model to variations in the gating function dynamics.

To do that, we altered the baseline dynamics of the gating function to have a slower characteristic decay time and a slower rate of accumulation; for example, we can set $\tau_f = 40sec$ and $\kappa = 0.1sec^{-1}$. Simulations show that the only effect is a slight blurring of the transition between different phases of the bursting, as would be expected. This can best be detected by looking at the distribution of inter-spike-interval increments, for the case of slow gating dynamics. The distribution, shown in Fig. 7, has weaker tail as compared to the distribution obtained for the faster gating dynamics. This result follows because for a slower gating, the modulation of the post-synaptic current is weaker. Hence, the transitions from intense firing to low-frequency spiking are less abrupt, resulting in a relatively low proportion of large increments. It is worth remembering that large increments of inter-spike intervals reflect sudden changes in dynamics which are eliminated by the blurring. Clearly, the model with fast gating does a better job in fitting the spiker data.

The time-dependent background current: All of the main results

were obtained under the assumption of constant background current feeding into neuronal soma, such that when acting alone, this current forces the model neuron to fire at some very low frequency. One may justly argue that there is no such thing as constant current. Indeed, if a background current has to do with the biological reality, then it should possess some dynamics. For example, a better match would be to imagine the background current to be associated with the activity in adjacent astrocytes (see e.g. [33]).

To test this, we simulated glia-gated autaptic neuron subject to slowly oscillating ($T = 10\text{sec}$) background current. For this case, we found that the behavior of a model is generically the same. Yet, now the transitions between the bursting phases are sharper (see Fig. 8a). This, in turn, leads to the sharper modulation of post-synaptic currents (shown in Fig. 8d). We can confirm this by noting that the distribution of inter-spike interval increments has a slightly heavier tail, as compared to the distribution obtained for the case of constant background current (data not shown). On the other hand, replacing the constant current with the oscillating one, introduces a typical frequency, not seen in the actual spiker data. This artificial problem will presumably disappear when the background current is determined self-consistently as part of the overall network activity. Similarly, the key to extending the increments distributions to longer time scales seems to be getting the network feedback to the spikers to regulate the inter-burst timing which at the moment is too regular. This will be presented in a future publication.

Discussion

In this paper, we have proposed that the regulation of synaptic transmission by astrocytic calcium dynamics is a critical new component of neural circuitry. We have used existing biophysical experiments to construct a coupled synapse-astrocyte model to illustrate this regulation and to explore its consequences for an autaptic oscillator, arguably the most elementary neural circuit. Our results can be compared to data taken from cultured neuron networks. This comparison reveals that the glial “gate-keeping” effect appears

to be necessary for an understanding of the inter-spike interval distribution of observed rapidly-firing “spiker” neurons, for time scales up to about 100msec.

Of course, many aspects of our modelling are quite simplified as compared to the underlying biophysics. We have investigated the sensitivity of our results to the modification of some of the parameters of our model as well as the addition of more complex dynamics for the various parts of our system. Our results with regard to the inter-spike interval are exceedingly robust.

This work should be viewed as a step towards understanding the full dynamical consequences brought about by the strong reciprocal couplings between synapses and the glial processes that envelop them. We have focused on the fact that astrocytic emissions shut down synaptic transmission when the activity becomes too high. This mechanism appears to be a necessary part of the regulation of spiker activity; without it, spikers would fire too often, too regularly. Related work by Nadkarni and Jung (private communication) focuses on a different aspect, that of increased fidelity of synaptic release (for otherwise highly stochastic synapses) due to glia-mediated increases in pre-synaptic calcium levels. As our working assumption is that the spikers are most likely to be neurons with “faithful” autapses, this effect does not play a role in our attempt to compare to the experimental data. It will of course be necessary to combine these two different pieces to obtain a more complete picture.

As stressed here, the application to spikers is just one way in which our new synaptic dynamics may alter our thinking about neural circuits. This particular application is appealing and informative but must at the moment be considered an untested hypothesis. Future experimental work must test the assumption that spikers have significant excitatory autaptic coupling, that pharmacological blockage of the synaptic current reverts their firing to low frequency almost periodic patterns, and that cutting the feedback loop with the enveloping astrocyte eliminates the heavy-tail increment distribution. Work towards achieving these tests is ongoing.

In the experimental system, a purported autaptic neuron is a part of active network and would therefore receive input currents from the other neurons in the network. This more complex input would clearly alter the

very-long-time inter-spike interval distribution, especially given the existence of a new *inter-burst* timescale in the problem. Similarly, the current approach of adding a constant background current to the neuron is not realistic; the actual background current, due to such processes as glial-generated currents in the cell soma, would again alter the long-time distribution. Preliminary tests have shown that these effects could extend the range of agreement between autaptic oscillator statistics and experimental measurements.

Just as the network provides additional input for the spiker, the spiker provides part of the stimulation that leads to the bursting dynamics. Future work will endeavor to create a fully self-consistent network model to explore the overall activity patterns of this system. One issue that needs investigation concerns the role that glia might have in coordinating the action of neighboring synapses. It is well-known that a single astrocytic process might contact thousands of synapses; if the calcium excitation spreads from being a local increase in a specific terminus to being a more widespread phenomenon within the glial cell body, neighboring synapses can become dynamically coupled. The role of this extra complexity in shaping the burst structure and time sequence is as yet unknown.

Acknowledgements

The authors would like to thank Gerald M. Edelman for insightful conversation about the possible role of glial cells. Eugene Izhikevich, Peter Jung, Suhita Nadkarni, Mark Shein, Nadav Raichman and Itay Baruchi are acknowledged for useful comments and for the critical reading of an earlier version of this manuscript. Vladislav Volman thanks the Center for Theoretical Biological Physics for hospitality. This work has been supported in part by the NSF-sponsored Center for Theoretical Biological Physics (grant numbers PHY-0216576 and PHY-0225630), by Maguy-Glass Chair in Physics of Complex Systems.

Parameters used in simulations

P_0	0.5	η_{mean}	$1.2 \cdot 10^{-3} \mu A cm^{-2}$	σ	0.1
τ_{ca}	4sec	κ	$0.5 sec^{-1}$	τ_{IP_3}	7sec
r_{IP_3}	$7.2 mM sec^{-1}$	IP_3^*	$0.16 \mu M$	c_1	0.185
v_1	$6 sec^{-1}$	v_2	$0.11 sec^{-1}$	v_3	$0.9 \mu M sec^{-1}$
k_3	$0.1 \mu M$	d_1	$0.13 \mu M$	d_2	$1.049 \mu M$
d_3	$0.9434 \mu M$	d_5	$0.08234 \mu M$	a_2	$0.2 \mu M^{-1} sec^{-1}$
c_0	$2.0 \mu M$	g_{Ca}	$1.1 mScm^{-2}$	g_K	$2.0 mScm^{-2}$
g_L	$0.5 mScm^{-2}$	V_{Ca}	100mV	V_K	-70mV
V_L	-35mV	V_1	-1mV	V_2	15mV
V_3	10mV	V_4	14.5mV	ϕ	0.3
I_{base}	$0.34 \mu A cm^{-2}$	τ_d	10msec	τ_{rec}	100msec
u	0.1	A	$10 \mu A cm^{-2}$		

References

- [1] A. Volterra and J. Meldolesi. Astrocytes, from brain glue to communication elements: the revolution continues. *Nat. Neurosci.*, 6:626–640, 2005.
- [2] P.G. Haydon. Glia: listening and talking to the synapse. *Nat. Rev. Neurosci.*, 2(3):185–193, 2001.
- [3] E.A. Newman. New roles for astrocytes: regulation of synaptic transmission. *Trends in Neurosci.*, 26(10):536–542, 2003.
- [4] T. Takano, G.F. Tian, W. Peng, N. Lou, W. Libionka, X. Han, and M. Nedergaard. Astrocyte-mediated control of cerebral blood flow. *Nat. Neurosci.*, 9(2):260–267, 2006.
- [5] A. Araque, V. Parpura, R.P. Sanzgiri, and P.G. Haydon. Tripartite synapses: glia, the unacknowledged partner. *Trends in Neurosci.*, 22(5):208–215, 1999.
- [6] G. Perea and A. Araque. Communication between astrocytes and neurons: a complex language. *J. Physiol.*, 96:199–207, 2002.

- [7] A.H. Cornell-Bell, S.M. Finkbeiner, M.S. Cooper, and S.J. Smith. Glutamate induces calcium waves in cultured astrocytes: long-range glial signaling. *Science*, 247:470–473, 1990.
- [8] A.C. Charles, J.E. Merrill, E.R. Dirksen, and M.J. Sanderson. Inter-cellular signalling in glial cells: calcium waves and oscillations in response to mechanical stimulation and glutamate. *Neuron*, 6:983–992, 1991.
- [9] A.H. Cornell-Bell and S.M. Finkbeiner. Ca²⁺ waves in astrocytes. *Cell Calcium*, 12:185–204, 1991.
- [10] S. Nadkarni and P. Jung. Spontaneous oscillations of dressed neurons: a new mechanism for epilepsy ? *Phys. Rev. Lett.*, 91(26), 2004.
- [11] J. Sneyd, B.T.R. Wetton, A.C. Charles, and M.J. Sanderson. Intercellular calcium waves mediated by diffusion of inositol triphosphate: a two-dimensional model. *Am. J. Physiol.*, 268:C1537–C1545, 1995.
- [12] T. Hofer, L. Venance, and C. Giaume. Control and plasticity of inter-cellular calcium waves in astrocytes. *J. Neurosci.*, 22:4850–4859, 2003.
- [13] A. Araque, V. Parpura, R.P. Sanzgiri, and P.G. Haydon. Glutamate-dependent astrocyte modulation of synaptic transmission between cultured hippocampal neurons. *Eur. J. Neurosci.*, 10(6):2129–2142, 1998.
- [14] A. Araque, V. Parpura, R.P. Sanzgiri, and P.G. Haydon. Glutamate-dependent astrocyte modulation of synaptic transmission between cultured hippocampal neurons. *J. Neurosci.*, 18(17):6822–6829, 1998.
- [15] G. Perea and A. Araque. Properties of synaptically evoked astrocyte calcium signal reveal synaptic information processing by astrocytes. *J. Neurosci.*, 25:2192–2203, 2005.
- [16] M.M. Segal. Epileptiform activity in microcultures containing one excitatory hippocampal neuron. *J. Neuroanat.*, 65:761–770, 1991.

- [17] M.M. Segal. Endogenous bursts underlie seizurelike activity in solitary excitatory hippocampal neurons in microculture. *J. Neurophysiol.*, 72:1874–1884, 1994.
- [18] J.M. Bekkers and C.F. Stevens. Excitatory and inhibitory autaptic currents in isolated hippocampal neurons maintained in cell culture. *Proc. Nat. Acad. Sci.*, 88:7834–7838, 1991.
- [19] R. Segev, M. Benveniste, E. Hulata, N. Cohen, A. Paleski, E. Kapon, Y. Shapira, and E. Ben-Jacob. Long term behavior of lithographically prepared in-vitro neural networks. *Phys. Rev. Lett.*, 88:118102, 2002.
- [20] E. Hulata, R. Segev, Y. Shapira, M. Benveniste, and E. Ben-Jacob. Detection and sorting of neural spikes using wavelet packets. *Phys. Rev. Lett.*, 85:4637–4640, 2000.
- [21] R. Segev and E. Ben-Jacob. Spontaneous synchronized bursting activity in 2d neural networks. *Physica A*, 302:64–69, 2001.
- [22] M. Tsodyks, A. Uziel, and H. Markram. Synchrony generation in recurrent networks with frequency-dependent synapses. *J. Neurosci.*, 20, 2000.
- [23] J.T. Porter and K.D. McCarthy. Hippocampal astrocytes in situ respond to glutamate released from synaptic terminals. *J. Neurosci.*, 16(16):5073–5081, 1996.
- [24] Y. Li and J. Rinzel. Equations for inositol-triphosphate receptor-mediated calcium oscillations derived from a detailed kinetic model: A hodgkin-huxley like formalism. *J. Theor. Biol.*, 166:461–473, 1994.
- [25] A.P. Gandhi and C.F. Stevens. Three modes of synaptic vesicular release revealed by single-vesicle imaging. *Nature*, 423:607–613, 2003.
- [26] Q. Zhang, T. Pangrsic, M. Kreft, M. Krzan, N. Li, J.Y. Sul, M. Halassa, E. van Bockstaele, R. Zorec, and P.G. Haydon. Fusion-related release of glutamate from astrocytes. *J. Biol. Chem.*, 279:12724–12733, 2004.

- [27] Y. Otsu, V. Shahrezaei, B. Li, L.A. Raymond, K.R. Delaney, and T.H. Murphy. Competition between phasic and asynchronous release for recovered synaptic vesicles at developing hippocampal autaptic synapses. *J. Neurosci.*, 24(2):420–433, 2004.
- [28] C. Morris and H. Lecar. Voltage oscillations in the barnacle giant muscle fiber. *Biophys. J.*, 35:193–213, 1981.
- [29] J. Kang, L. Jiang, S.A. Goldman, and M. Nedergaard. Astrocyte-mediated potentiation of inhibitory synaptic transmission. *Nat. Neurosci.*, 1:683–692, 1998.
- [30] H.S. Seung, D.D. Lee, B.Y. Reis, and D.W. Tank. The autapse: a simple illustration of short-term analog memory storage by tuned synaptic feedback. *J. Comp. Neurosci.*, 9:171–185, 2000.
- [31] J. Lubke, H. Markram, M. Frotscher, and B. Sakmann. Frequency and dendritic distributions of autapses established by layer-5 pyramidal neurons in developing rat cortex. *J. Neurosci.*, 16:3209–3218, 1996.
- [32] J.W. Shuai and P. Jung. Langevin modelling of intra-cellular calcium dynamics, in: Understanding calcium dynamics - experiments and theory. *Lecture Notes in Physics*, eds. M. Falcke and D. Malchow. Springer, pages 231–252, 2003.
- [33] M.C. Angulo, A.S. Kozlov, S. Charpak, and E. Audinat. Glutamate released from glial cells synchronizes neuronal activity in the hippocampus. *J. Neurosci.*, 24(31):6920–6927, 2004.

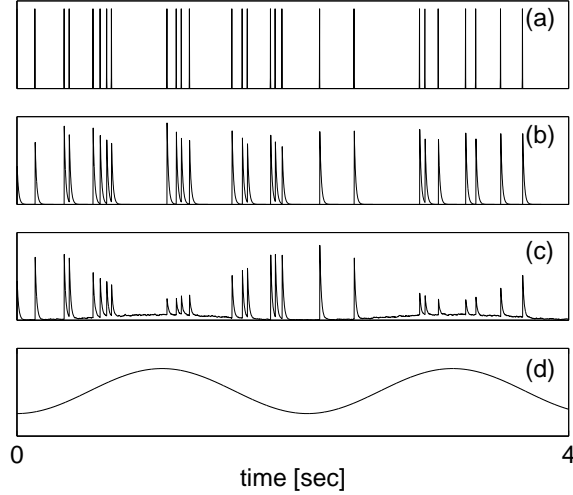


Figure 1: The generic effect of an astrocyte on the pre-synaptic depression, as captured by our phenomenological model (see text for details). To illustrate the effect of pre-synaptic depression and the astrocyte influence, we feed a model synapse with the input of spikes taken from the recorded activity of a cultured neuronal network (see main text and [21] for details). a) The input sequence of spikes that is fed into the model pre-synaptic terminal. b) Each spike arriving at the model pre-synaptic terminal results in the post-synaptic current (*PSC*). The strength of the post-synaptic current depends on the amount of available synaptic resources, and the synaptic depression effect is clearly observable during spike trains with relatively high frequency. c) The effect of a periodic gating function, $f(t) = 0.5 + f_0 \sin(wt)$, shown in (d). The period of the oscillation, $T = \frac{2\pi}{\omega} = 2\text{sec}$, is taken to be compatible with the typical time scales of variations in the intra-glial Ca^{2+} concentration. Note the reduction in the *PSC* near the maxima of f , along with the elevated base-line resulting from the increase in the rate of spontaneous pre-synaptic transfer.

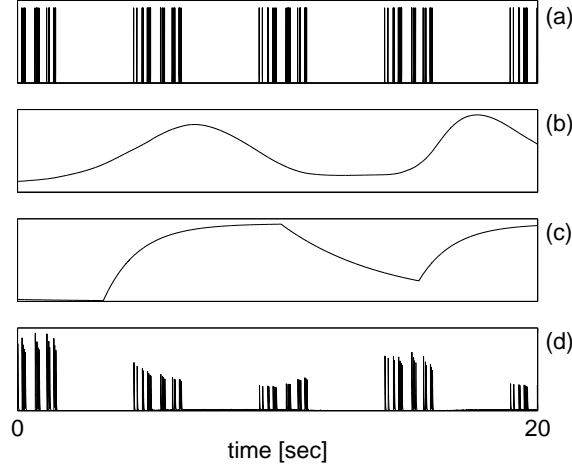


Figure 2: The "gate-keeping" effect in a glia-gated synapse. Top panel (a) shows the input sequence of spikes, which is composed of several copies of the sequence shown in figure 1, separated by segments of long quiescent time. The resulting time series may be viewed as bursts of action potentials arriving at the model pre-synaptic terminal. The first burst of spikes results in the elevation of free astrocyte Ca^{2+} concentration (shown in (b)), but this elevation alone is not sufficient to evoke oscillatory response. An additional elevation of Ca^{2+} , leading to the emergence of oscillation, is provided by the second burst of spikes arriving at the pre-synaptic terminal. Once the astrocytic Ca^{2+} crosses a pre-defined threshold, it starts to exert a modulatory influence back on the pre-synaptic terminal. In the model, this is manifested by the rising dynamics of the gating function (shown in (c)). Note that, as the decay time of the gating function f is of the order of seconds, the astrocyte influence on the pre-synaptic terminal persists even after concentration of astrocyte Ca^{2+} has fallen. This is best seen from figure (d), where we show the profile of the post-synaptic current (PSC). The third burst of spikes arriving at the pre-synaptic terminal is modulated due to the astrocyte, even though the concentration of Ca^{2+} is relatively low at that time. This modulation extends also to the fourth burst of spikes, which together with the third burst leads again to the oscillatory response of astrocyte Ca^{2+} . Taken together, all of these results illustrate a temporally non-local "gate-keeping" effect of glia cells.

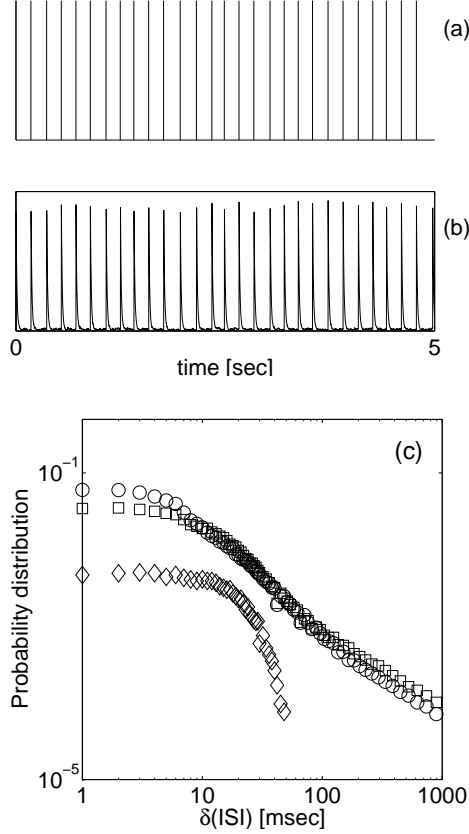


Figure 3: The activity of a model neuron containing the self-synapse (autapse), as modelled by the "classical" Tsodyks-Uziel-Markram model of synaptic transmission. In this case, it is possible to recover some of the features of cortical rapidly-firing neurons, namely the relatively high-frequency persistent activity. However, the resulting time-series of action potentials for such a model neuron, shown in (a), is almost periodic. Due to the self-synapse, a periodic series of spikes results in the periodic pattern for the post-synaptic current (shown in (b)), which closes the self-consistency loop by causing a model neuron to generate a periodic time-series of spikes. Further difference between the model neuron and between cortical rapidly-firing neurons is seen upon comparing the corresponding distributions of ISI increments, plotted on double-logarithmic scale. These distributions, shown in (c), disclose that, contrary to the cortical rapidly-firing neurons, the increments distribution for the model neuron with TUM autapse (diamonds) is Gaussian (seen as a "stretched" parabola on double-log scale), pointing at the existence of characteristic time-scale. On the other hand, distributions for cortical neurons (squares and circles) decay algebraically and are much broader. The distribution of the model neuron has been vertically shifted, for clarity of comparison.

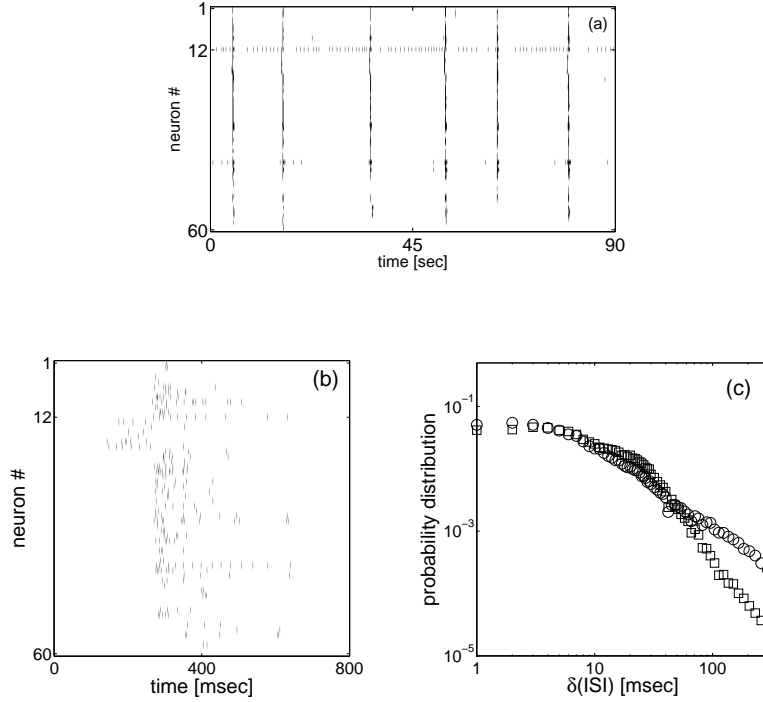


Figure 4: Electrical activity of *in-vitro* cortical networks. These cultured networks are spontaneously formed from a dissociated mixture of cortical neurons and glial cells drawn from one-day-old Charles River rats. The cells are homogeneously spread over a lithographically specified area of Poly-D-Lysine for attachment to the recording electrodes. The activity of a network is marked by formation of synchronized bursting events (*SBEs*), short ($\sim 100 - 400\text{msec}$) periods of time during which most of the recorded neurons are active. a) A raster plot of recorded activity, showing a sample of few *SBEs*. The time axis is divided into 10^{-1}s bins. Each row is a binary barcode representation of the activity of an individual neuron, i.e. the bars mark detection of spikes. Note that, while majority of the recorded neurons are firing rapidly mostly during *SBEs*, there are some neurons that are marked by persistent intense activity (for example neuron no.12). This property supports the notion that the activity of these neurons is autonomous and hence self-amplified. b) A zoomed view of a sample synchronized bursting event. Note that each neuron has its own pattern of activity during the *SBE*. To access the differences in activity between ordinary neurons and neurons that show intense firing between the *SBEs*, for each neuron we constructed the series of increments of inter-spike intervals (ISI), defined as $\delta(i) = ISI(i+1) - ISI(i), i \geq 1$. The distributions of $\delta(i)$, shown in (c), disclose that the dynamics of ordinary neurons (squares) is similar to the dynamics of rapidly firing neurons (circles), up to the time-scale of 100msec, corresponding to the width of a typical *SBE*. Note that since *increments* of inter-spike-intervals are analyzed, the increased rate of neurons firing does not necessarily affect the shape of the distribution. Yet, above the characteristic time of 100msec, the distributions diverge, possibly indicating the existence of additional mechanisms governing the activity of rapidly-firing neurons on a longer time-scale. Note that for normal neurons there is another peak at typical inter-burst intervals ($> \text{seconds}$), not shown here.

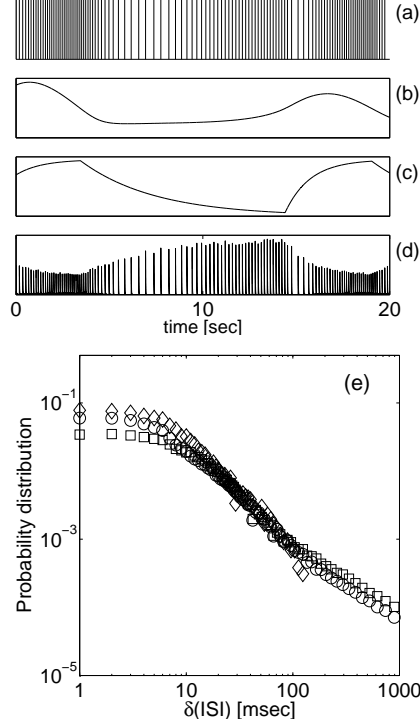


Figure 5: The activity of a model neuron containing a glia-gated autapse. The equations of synaptic transmission for this case have been modified to take into account the influence of synaptically-associated astrocyte, as explained in text. The resulting spike time-series, shown in (a), deviates from periodicity due to the slow modulation of the synapse by the adjacent astrocyte. The relatively intense activity at the pre-synaptic terminal activates astrocyte receptors, which in turn leads to the production of IP_3 and subsequent oscillations of free astrocyte Ca^{2+} concentration. The period of these oscillations, shown in (b), is much larger than the characteristic time between spikes arriving at the pre-synaptic terminal. Because Ca^{2+} dynamics is oscillatory, so also will be the dynamics of the gating function f , as is seen from (c), and period of oscillations for f will follow the period of Ca^{2+} oscillations. The periodic behavior of f leads to slow periodic modulation of PSC pattern (shown in (d)), which closes the self-consistency loop by causing a neuron to fire in a burst-like manner. Additional information is obtained after comparison of distributions for ISI increments, shown in (e). Contrary to results for the model neuron with a simple autapse (see figure 4c), the distribution for a glia-gated autaptic model neuron (diamonds) now closely follows the distributions of two sample recorded cortical rapidly-firing neurons (squares and circles), up to the characteristic time of $\sim 100msec$, which corresponds to the width of a typical SBE. The heavy tails of the recorded distributions above this characteristic time indicate that network mechanisms are involved in shaping the form of the distribution on longer time-scales.

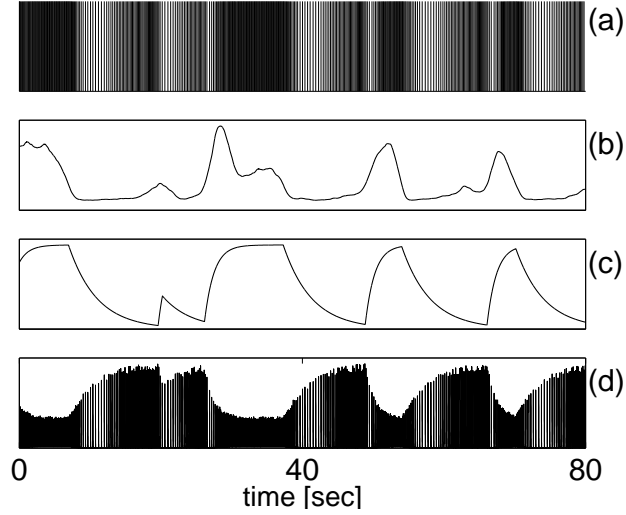


Figure 6: The dynamical behavior of an astrocyte-gated model autaptic neuron, including the stochastic release of calcium from ER of astrocyte. Shown are the results of the simulation when calcium release from intra-cellular stores is mediated by a cluster of $N=10$ channels. The generic form of the spike time-series (shown in (a)) does not differ from those obtained for the deterministic model. Namely, even for the stochastic model the neuron is still firing in a burst-like manner. Although the temporal profile of astrocyte calcium (b) is irregular, the resulting dynamics of the gating function (c) is relatively smooth, stemming from the choice of the gating function dynamics (being an integration over the calcium profile). As a result, the PSC profile (shown in d) does not differ much from the corresponding PSC profile obtained for the deterministic model.

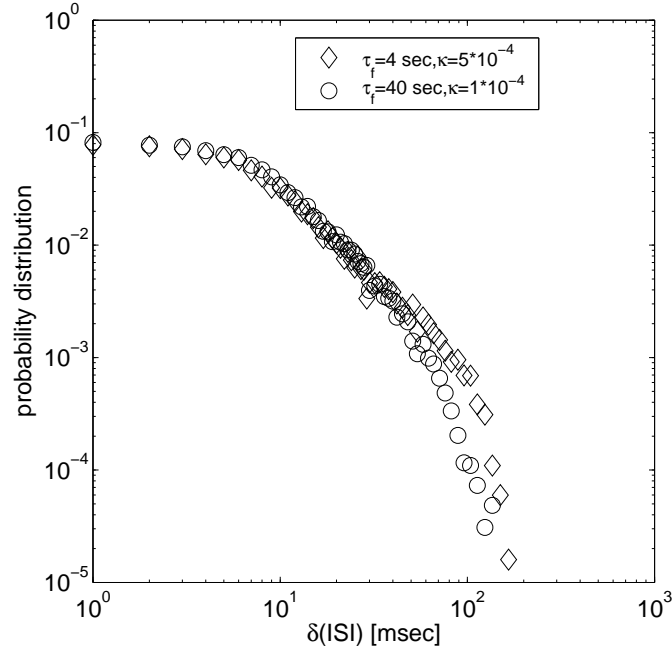


Figure 7: Distributions of inter-spike-interval increments for the model of an astrocyte-gated autaptic neuron with slow dynamics of the gating function, as compared with the corresponding distribution for the deterministic Li-Rinzel model. Due to the slow dynamics of the gating function, the transitions between different phases of bursting are blurred, resulting in a weaker tail for the distribution of inter-spike interval increments.

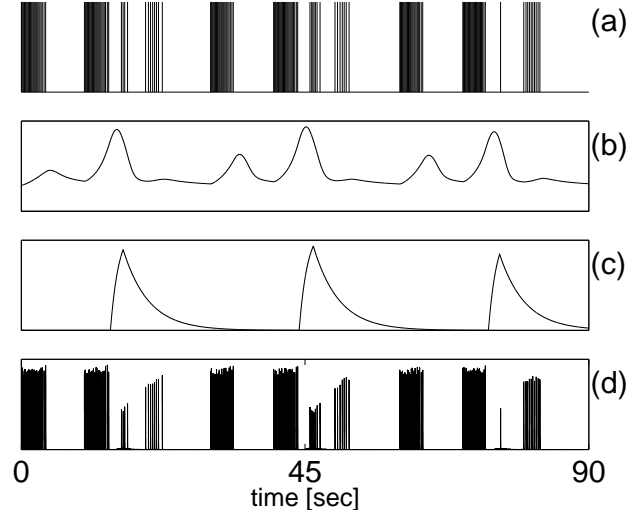


Figure 8: The dynamical behavior of an astrocyte-gated model autaptic neuron with slowly oscillating background current. Shown are the results of the simulation when $I_{base} \propto \sin(\frac{2\pi}{T}t)$, $T = 10sec$. The mean level of I_{base} is set so as to put a neuron in the quiescent phase for half a period. The resulting spike time-series (shown in a) disclose the burst-like firing of a neuron, with the super-imposed oscillatory dynamics of a background current. The variations in the concentration of astrocyte calcium (b) are much more temporally localized, and so is the resulting dynamics of the gating function (shown in c). Consequently, the PSC profile (d) strongly reflects the burst-like synaptic transmission efficacy, thus forcing the neuron to fire in a burst-like manner and closing the self-consistency loop.